SLAC-PUB-6323
SLAC/SSRL-0046
August 1993
(SSRL-M)

TESTS OF PLANAR PERMANENT MAGNET MULTIPOLE FOCUSING ELEMENTS*

J. Cobb and R. Tatchyn

Stanford Linear Accelerator Center, Stanford Synchrotron Radiation Laboratory,
Stanford University, Stanford, California 94309

Abstract

In recent work, planar configurations of permanent magnets were proposed as substitutes for conventional current-driven iron quadrupoles in applications limited by small aperture sizes and featuring small beam occupation diameters. Important examples include the configuring of focusing lattices in small-gap insertion devices, and the implementation of compact mini-beta sections on linear or circular machines. In subsequent analysis, this approach was extended to sextupoles and higher-order multipoles. In this paper we report on initial measurements conducted at the Stanford Linear Accelerator Center on recently fabricated planar permanent magnet quadrupoles and sextupoles configured out of SmCo and NdFe/B.

Presented at the 8th National Conference on Synchrotron Radiation Instrumentation,
Gaithersburg,Md, August 23-26, 1993

---

*Supported by DOE Offices of Basic Energy Sciences and High Energy and Nuclear Physics and Department of Energy Contract DE-AC03-76SF0015.

1. Introduction

Magnetic quadrupoles and sextupoles are among the most widely used focusing and aberration-correcting elements in present-day particle-beam transport and accelerating systems [1]. The predominant implementations consist of rotationally symmetric iron yokes with specially shaped poles excited by current windings. A typical quadrupole, for example, features four salient poles with surfaces contoured as hyperbolic cylinder sections, with an outside cylindrical support/flux-return that completely surrounds the particle beam axis. Permanent magnet (PM) structures with the same general symmetry and similar material or field distributions have also been designed [2] and employed. Due to the emphasis on rotational symmetry, such structures feature the property that their field distributions at relatively large distances from the symmetry axis remain dominated by the primary multipole components after which they are named. This property can be highly advantageous, for example, in the analysis or design of complex focusing lattices with large dynamic apertures, viz., through which the particle motion exhibits large off-axis deviations. Notwithstanding this, situations can arise in which the use of structures that completely enclose the particle axis can present impediments to effective lattice design and operation. Two important examples include: 1) the design of focusing (e.g., FODO) lattices for small-gap insertion devices; and 2) the implementation of compact optics with lateral access to the particle beam for diagnostic purposes. In recent work, for example, both situations were encountered in the design of a 1.5 cm gap, 60 m long PM undulator for the proposed 4 nm Free Electron Laser (FEL) project at SLAC [3]. In view of the fact that the size and positional drift of the particle beam through this device (viz., its occupation diameter) is expected to remain on the sub-100 μm level, an alternative, less symmetric configuration for the usual focusing quadrupole was proposed [4]. This configuration, consisting of four identically fabricated and magnetized rectangular PMs, with the easy axis normal to two of the faces, is shown in front view on the left hand side of Fig. 1. It is evident from the indicated field vectors that an approximation to a conventional quadrupole field distribution can be obtained by suitably separating the vertical PM pairs in the horizontal direction followed by 45 degree rotations of the individual pieces. The proposed (x-y) field distribution can consequently be viewed as a conventional quadrupole with superimposed unequal field distributions induced in the horizontal vs. vertical directions. Apart from the unconventional field distribution, a number of potentially advantageous features are also apparent. These include: 1) a fully open horizontal aperture; 2) a low vertical profile, in particular when the height of the PM pieces is small; 3) maximal ease of fabrication and magnetization; 4) flexible design and implementation of focusing lattices; and 5) the possible attainment of large focusing gradients with small

amounts of PM material. In subsequent work , the basic notion of the planar PM quadrupole has been extended to sextupole and higher order multipole structures [5]. An example of a planar PM sextupole is depicted on the right side of Fig. 1.

Due to the compactness and simple geometry of these elements, a number of novel control and design options of practical interest suggest themselves [4]. For example, a method for tuning their fields by placing permeable sheets in proximity to their top and bottom surfaces has been considered. The induced image fields modulate the multipole components of the free-space distribution, enhancing the quadrupole component with minimal perturbation of the higher multipole components. More generally, it can be shown that replacing the (plane) sheets with more arbitrary permeable material distributions possessing left-right symmetry will also modulate the free-space components without introducing any new ones. In configuring focusing (e.g., FODO) lattices, this important property allows the installation of planar PM elements into the gaps of many different classes of undulators: pure-PM, hybrid, PM-free electromagnetic, iron-free electromagnetic, and others, including devices featuring non-magnetic fields. In undulators with permeable poles, the primary requirement is that the pole surfaces exhibit shapes and magnetic property distributions with the appropriate left-right symmetry. In configurations where both the undulator and focusing lattice are pure PM, it becomes possible to consider tuning the primary undulator field by the method of induced images, a potentially attractive option for ultra-long undulators in which jaw motion is impracticable, and whose required tuning range is less than an octave. With respect to these and other possibilities, the planar PM multipoles can be seen to contribute a significantly increased design flexibility for controlling both the spectral and particle-focusing properties of insertion devices [6].

In recent months at the Stanford Linear Accelerator Center (SLAC), we have initiated a systematic series of measurements of various practical implementations of the planar PM quadrupole (quad) and sextupole. In particular, we have: 1) characterized their free-space distributions; 2) determined the effects of permeable planes on their free-space fields; 3) installed a PM quadrupole into the gap of a prototype section of the hybrid electromagnetic undulator PALADIN [7] and measured the total field in the vicinity of the axis with the prototype fields both on and off. In this paper we issue our first report on these tests and provide comparisons of selected measurement results with analytical calculations.

2. Field distributions

The potential associated with each of the structures in Fig. 1 in proximity to the axis ($x = y = 0$) can be

expanded in a real Taylor series whose terms can be associated with the field multipole components [5]. For the PM quadrupole, we have

$$\phi_Q(x,y) = C_{11}xy + E_{13}(xy^3 - x^3y) + \ldots, \tag{1}$$

with

$$C_{11} = \frac{-2B_r}{\pi}\left[\frac{w^2}{g'\left(w^2+g'^2\right)}\right]_{g'=h+(g/2)}^{g'=(g/2)}, \tag{2}$$

and

$$E_{13} = \frac{2B_r}{3\pi}\left[\frac{w^2(6g'^4+3w^2g'^2+w^4)}{g'^3\left(w^2+g'^2\right)^3}\right]_{g'=h+(g/2)}^{g'=(g/2)}, \tag{3}$$

where B_r[T] is the PM's remanent field. Evidently, the field gradients are given by

$$\frac{\partial B_x(x,y,0)}{\partial y} = \frac{\partial B_y(x,y,0)}{\partial x} = C_{11} + 3E_{13}(y^2 - x^2) + \ldots, \tag{4}$$

where C_{11} represents the dominant quadrupole field component, and the next term indicates the (antisymmetric in x vs y) octupole component. In this form, the coefficient E_{13} reflects the strength with which the horizontally vs vertically uneven distribution of PM material induces corresponding field asymmetries in regions away from the axis. while the variable terms indicate that the planar PM quadrupole will closely approximate an ideal quadrupole in regions sufficiently close to the axis.

Expansion of the sextupole field yields similar results, with the exception that the lowest-order term represents a dipole field component. Thus,

$$\phi_S = B_{01}y + D_{21}(3x^2y - y^3) + F_{41}\left(5x^4y - 10x^2y^3 + y^5\right) + \ldots, \tag{5}$$

with

$$B_{01} = \frac{-2B_r}{\pi}\left[2\tan^{-1}\left(\frac{b}{g'}\right) - \tan^{-1}\left(\frac{a}{g'}\right)\right]_{g'=h+(g/2)}^{g'=(g/2)}, \tag{6}$$

and

$$D_{21} = \frac{2B_r}{3\pi}\left[\frac{2g'b}{\left(a^2+g'^2\right)^2} - \frac{ag'}{\left(b^2+g'^2\right)^2}\right]_{g'=h+(g/2)}^{g'=(g/2)} \quad (7)$$

Evidently, to create a field with a leading sextupole component, the condition B_{01}=0 must be established.

3. Measurement apparatus and stand-alone PM multipole test results

A rotating-coil probe was designed and fabricated for the multipole tests. As shown in Fig. 2, it consists of a rectangular 2 mm x 1 cm coil with one of its long sides set on the symmetry (rotation) axis. The outer side consequently rotates on a cylindrical surface with an average 2 mm radius. At a constant rotation frequency of 30 Hz, a harmonic decomposition of the signal reveals the fundamental (constant) quadrupole component and the higher multipole components along the 2 mm circumference of rotation. The magnitudes of the field components are unfolded from the rotation rate and a knowledge of the coil's geometry and electrical parameters.

A number of planar PM multipoles were designed at the Stanford Synchrotron Radiation Laboratory (SSRL) and the individual rectangular pieces fabricated by Magnet Sales and Manufacturing, Inc. [8]. The geometric and field parameters of the samples reported on in this paper are listed in Table 1. The machining dimensions on all the pieces were specified with ±0.025 mm tolerances. To take advantage of the symmetries of the given structures in optimizing field quality, the manufacturer was instructed to cut the material for each multipole out of a single source piece and machine it to the required dimensions prior to cutting it into the constituent pieces. The remanent field was specified to lie in the 1-1.2 T range, with the constituent pieces of each multipole to be magnetized in the same field. The multipole units were assembled by hand at the Magnetic Measurements facility at SLAC and affixed to specially designed and machined (±0.025 mm) brass fixtures with ordinary cement. Front views of the experimental configurations for measuring the PM quadrupole and sextupole fields tuned by the method of images are schematized in Fig. 3.

A typical rotating-coil measurement spectrum is shown for Sample 1 in Fig. 4. Although these spectra extend out to the dodecapole (12-pole) component for the quadrupoles and the 14-pole component for the sextupole, for this initial report we have restricted our analysis to the C_{11} and E_{13} terms for the quad and the B_{01} and D_{21} for the sextupole. The calculated vs measured multipole field components are listed in

Table 2. The remanent field values listed in the table, which were calculated from the dominant field components of the measured spectra, were presumed to represent the actual magnetization fields. Thus, the calculated values in the table have been scaled to establish agreement between the measured and calculated dominant field components in the "free-space" configurations. The principal error sources are associated with the tolerances on the coil dimensions, errors in positioning and alignment of the coil axis with respect to the symmetry axis of the multipoles, and PM positional errors associated with their assembly. The net contribution of these errors to the variation in the measured field amplitudes, as well as in the observed ratios among them, is estimated to be ± 5 %. With respect to these error specifications and the data scaling, Sample 1 (the NdFe/B quad) is seen to agree closely with calculations, while a significant (approximately 20 %) discrepancy is apparent in the measured vs calculated octupole components of Sample 2 (SmCo). The sextupole's dipole component in the free-space case is evidently not fully nulled, and appears as an effective offset component both here and in the image tuned case. As discussed in detail in prior work [6], the sensitivity of the associated B_{01} coefficient to positional errors and induced image fields is strongly corroborated.

4. Tests of a PM quadrupole installed in a prototype PALADIN section

A potentially important application of the planar PM multipoles is to configure superimposed focusing or aberration-correcting fields over the primary fields of insertion devices or other machine elements. In the case of Free-Electron Laser (FEL) insertion devices, enhanced focusing can significantly improve the attainable gain for a given undulator length [9]. For example, recent investigations by the SLAC FEL research group [10] have indicated that increasing the K value and focusing strength of the PALADIN undulator would make it possible to reduce the wavelength at which Self Amplified Spontaneous Emission (SASE) saturation (in the available 25 m) could be attained from 120 nm down to about 40 nm. With this and similar applications in mind, the feasibility of installing and operating a PM planar quadrupole in the aperture of a prototype section of PALADIN was investigated. The configuration of the magnetic cell of PALADIN is shown in the left side of Fig. 5. Its existing sextupole focusing [11] is determined by the gap and geometry of the concave cutouts in the pole faces. As indicated in the right hand side of Fig. 5, the aperture provided by these cutouts allows sufficient room to install a relatively strong-field planar PM quadrupole with a resulting vertical 1 cm gap. In our initial characterization, we: 1) measured the B_y field component in the x-direction with no quadrupole in the aperture and the peak field amplitude set to about

0.5 T; 2) installed a NdFe/B quadrupole (Sample 1) into PALADIN's gap on a specially prepared brass support and took a scan of its field in the x direction with the prototype's field turned off; and 3) took the same x-scan with the field turned back to 0.5 T. The results of these scans are presented in Fig. 6. Numerical analysis of the different curves indicates that, to within about 1 %, the fields of PALADIN and the 57 T/m PM quadrupole superpose linearly. The magnitude of this discrepancy can be fully accounted for by our systematic experimental errors, in particular positioning errors arising from the strong torque exerted on the quad by PALADIN's primary field. It should be noted, however, that effects related to the interaction of the poles' and quad's fields with the yoke poles running in a non-linear permeability regime (viz., with effective breaking of the required left-right symmetry) could also account for some part of the discrepancy, although in the present case this effect can be estimated to be small. The measured gradient of the PM quadrupole installed in PALADIN is found to be larger than its free-space value, as could be expected from the relative proximity of the steel pole surfaces to the PM material (see right hand drawing in Fig. 5).

5. Discussion

The use of planar PM multipoles in particle accelerator and insertion device design represents a promising direction for future development. Given the wide range of parameter space represented by the freedom of varying the height, length, and remanent field of the multipoles, enhanced flexibility in the design of focusing or aberration-correcting lattices can be achieved. The present work indicates that design and fabrication of very compact PM elements with high field gradients (of the order of 100 T/m in a 1 cm gap) and high quality fields is feasible. An assessment of all the data also suggests that care must be taken to control the quality and precision of assembly of the individual PM pieces utilized in multipole construction. For example, the observed discrepancy in the SmCo data needs to be further investigated, primarily by characterizing the fields of the individual pieces in more detail. With regard to questions concerning the apparently limited tunability of the PM multipoles with the image-field method, a comprehensive discussion of alternative tuning methods with greater dynamic ranges has been published elsewhere [5]. An important reason for focusing on the image method in the present work is that it is directly relevant to the concept of inserting the multipoles into structures with permeable pole faces. For example, it is evident from the increase of the PM sextupole's dipole component with the steel plates present (Table 2) and the field equations in Section 2 that it should be possible to compute sextupole

dimensions for which $B_{01}\neq 0$, but for which the net sum of the B_{01} coefficients of the structure and its induced images reduces to zero.

In general, two physical effects will tend to limit the quality and reduction in size of the PM multipoles. The first relates to the fact that the relative error associated with a fixed mechanical tolerance will increase inversely with the size of the structure. The second follows from the discontinuous nature of magnetic domain boundaries at small scales of size. In particle-beam applications requiring dominant quadrupole or sextupole fields over definite diameters, reduction of the multipole segment sizes will also be limited by the minimal gap at which the field in the defined region retains the desired quality. Up to these limits, however, it is evident that the use of the proposed structures can encompass a much wider range of parameter space than conventional current-driven devices.

6. Acknowledgments

We thank Ted Scharlemann for permission to include the drawing of PALADIN's cell structure in Fig. 5. This research was performed at SSRL and SLAC, which are operated by the Department of Energy, Offices of Basic Energy Sciences and High Energy and Nuclear Physics.

9

Table 1

Material, dimensional, and field parameters of PM planar multipole samples.

	NdFe/B Quadrupole (Sample 1)	SmCo Quadrupole (Sample 2)	NdFe/B Sextupole (Sample 3)
B_r(remanent field)	1-1.2 T	1-1.2 T	1-1.2 T
Length	3 cm	4 cm	3 cm
PM height	2.5 mm	5 mm	5 mm
Gap	1 cm	1 cm	1 cm
Width (side pieces)	1 cm	1 cm	2.633 mm
Width (central pieces)	-	-	3.2 mm

Table 2

Calculated vs. measured field components (gradients (T/m) for the quadrupole and amplitudesextupole) of PM planar multipole samples. Data taken at a radius of 2 mm.

	NdFe/B Quadrupole [a] (Sample 1)		SmCo Quadrupole [b] (Sample 2)		NdFe/B Sextupole [c] (Sample 3)	
	Free-space	Steel Plates	Free-space	Steel Plates	Free-space	Steel Plates
t*	-	2.67 mm	-	3.2 mm	-	0 mm
Quadrupole (calc.)	57.6	65.3	74.57	80.2	-	-
Quadrupole (meas.)	57.6	64.2	74.57	80.1	-	-
Octupole (calc.)	14.4	14.5	13.54	13.6	-	-
Octupole (meas.)	14.6	14.4	16.5	16.9	-	-
Dipole (calc.)	-	-	-	-	0	0.013
Dipole (meas.)	-	-	-	-	0.0031	0.0145
Sextupole (calc.)	-	-	-	-	0.0222	0.0239
Sextupole (meas.)	-	-	-	-	0.0222	0.0237

* distance between steel plates and top and bottom PM multipole surfaces.

a) B_r=1.2 T; b) B_r= 1.07 T; c) B_r=1.15 T

7. References

[1] E. Regenstreif, "Focusing with Quadrupoles, Doublets, and Triplets," in Focusing of Charged Particles, A. Septier, ed., Academic Press, New York, 1967, pp. 353-410.

[2] K. Halbach, "Design of Permanent Multipole Magnets with Oriented Rare Earth Cobalt Materials," Nuclear Instruments and Methods 169, 1(1980).

[3] R. Tatchyn, R. Boyce, K. Halbach, H.-D. Nuhn, J. Seeman, H. Winick, C. Pellegrini, "Design Considerations for a 60 Meter Pure Permanent Magnet Undulator for the SLAC Linac Coherent Light Source," Proceedings of the Particle Accelerator Conference (PAC'93), Washington, D. C., May 17-20, 1993, SLAC-PUB-6106.

[4] R. Tatchyn, "Permanent Magnet Edge-Field Quadrupoles As Compact Focusing Elements for Single-Pass Particle Accelerators," SLAC-PUB-6058.

[5] R. Tatchyn, "Planar Permanent Magnet Multipoles for Particle Accelerator and Storage Ring Applications," SLAC-PUB-6186, submitted to IEEE Trans. Mag., 1993.

[6] R. Tatchyn, "Selected Applications of Planar Permanent Magnet Multipoles in FEL Insertion Device Design," presented at the 1993 International FEL Conference, The Hague, Holland, August 23-27, 1993.

[7] G. A. Deis, "A Long Electromagnetic Wiggler for the PALADIN Free-Electron Laser Experiments," IEEE Trans. Mag. 24(2), 1090(1988).

[8] Location: 11248 Playa Court, Culver City, CA, 90230-8162.

[9] R. Tatchyn, "Optimal Insertion Device Parameters for SASE FEL Operation," Proceedings of the Workshop on Fourth Generation Light Sources, M. Cornacchia and H. Winick, eds., SSRL Report No. 92/02, p. 605.

[10] H. Winick, K. Bane, R. Boyce, J. Cobb, G. Loew, P. Morton, H.-D. Nuhn, J. Paterson, P. Pianetta, T. Raubenheimer, R. Tatchyn, J. Seeman, V. Vylet, C. Pellegrini, J. Rosenzweig, G. Travish, D. Prosnitz, E. T. Scharlemann, K. Halbach, K.-J. Kim, R. Schlueter, M. Xie, R. Bonifacio, L. DeSalvo, P. Pierini, "Short Wavelength FELs Using the SLAC Linac," - elsewhere these proceedings.

[11] E. T. Scharlemann, "Wiggle-plane focusing in linear wigglers," J. Appl. Phys. 58(6), 2154(1985).

8. Figure Captions

Figure 1. Front views of permanent magnet quadrupole (left) and sextupole (right) configurations with arbitrary parameters.

Figure 2. Rotating-coil apparatus for scanning PM multipole field distributions. The rotating head can be positioned at arbitrary locations along the z axis.

Figure 3. Experimental PM multipole samples in image-tuning geometries. For free space measurements, $t \rightarrow \infty$.

Figure 4. Rotating-coil spectra for free-space (top) and image-tuned (bottom) measurements. Field components sampled at a radius of 2 mm.

Figure 5. Detailed view of the magnetic cell structure of the PALADIN undulator (left), with a front view of PALADIN's yoke showing the (Sample 1) NdFe/B quadrupole installed concentrically wiith PALADIN's axis (right). In the experimental characterization of the yoke+quad fields, g=18 mm, and the quadrupole is centered in a plane containing the maximum value of B_y.

Figure 6. Scans of B_y (x) along the center of an x-y plane bisecting two opposed PALADIN poles, both with and without the installed quadrupole.

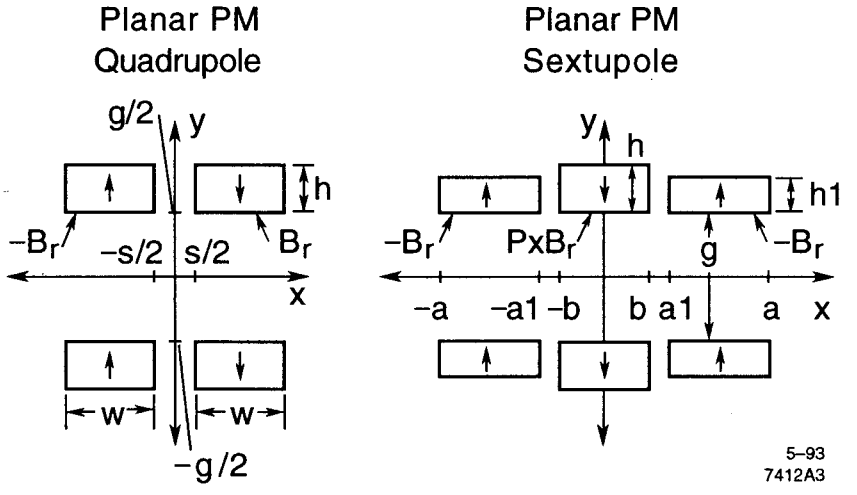
Planar PM
Quadrupole
g/2
y
h
$-B_r$
-s/2
s/2
B_r
x
w
w
-g/2
Planar PM
Sextupole
y
h
h1
$-B_r$
PxB_r
g
$-B_r$
-a
-a1
-b
b
a1
a
x
5-93
7412A3

Fig. 1

PM Planar Mutipole Field Measurement Apparatus

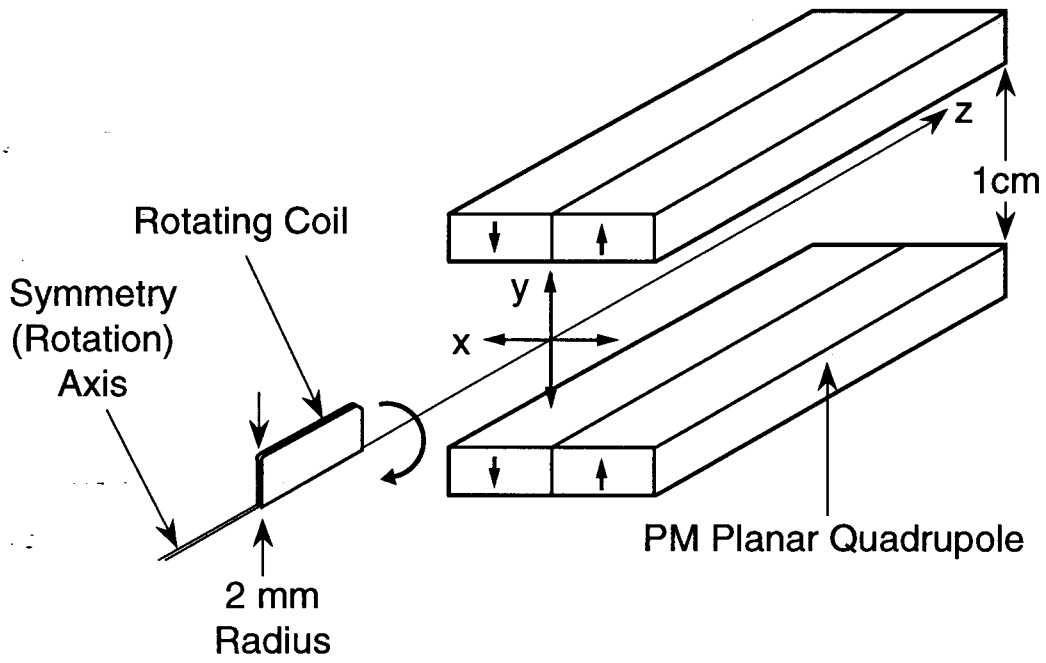

8-93

7523A2

Fig. 2

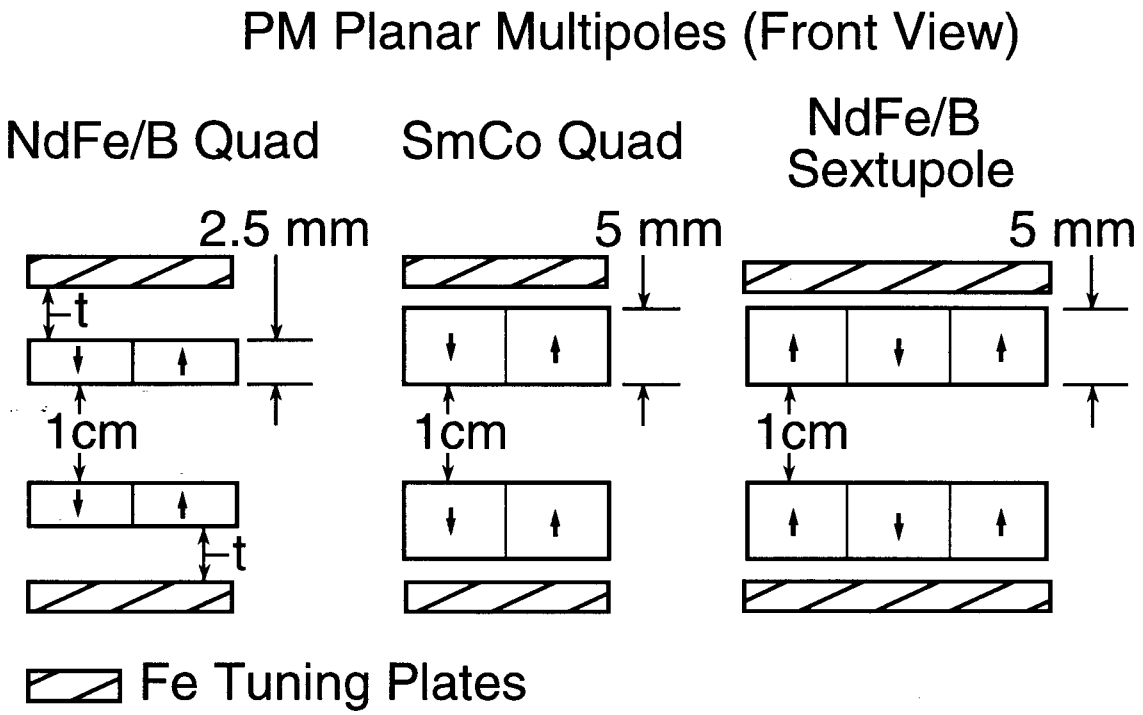
PM Planar Multipoles (Front View)
NdFe/B Quad
SmCo Quad
NdFe/B
Sextupole
2.5 mm
5 mm
5 mm
t
1cm
1cm
1cm
t
Fe Tuning Plates
8-93
7523A4

Fig. 3

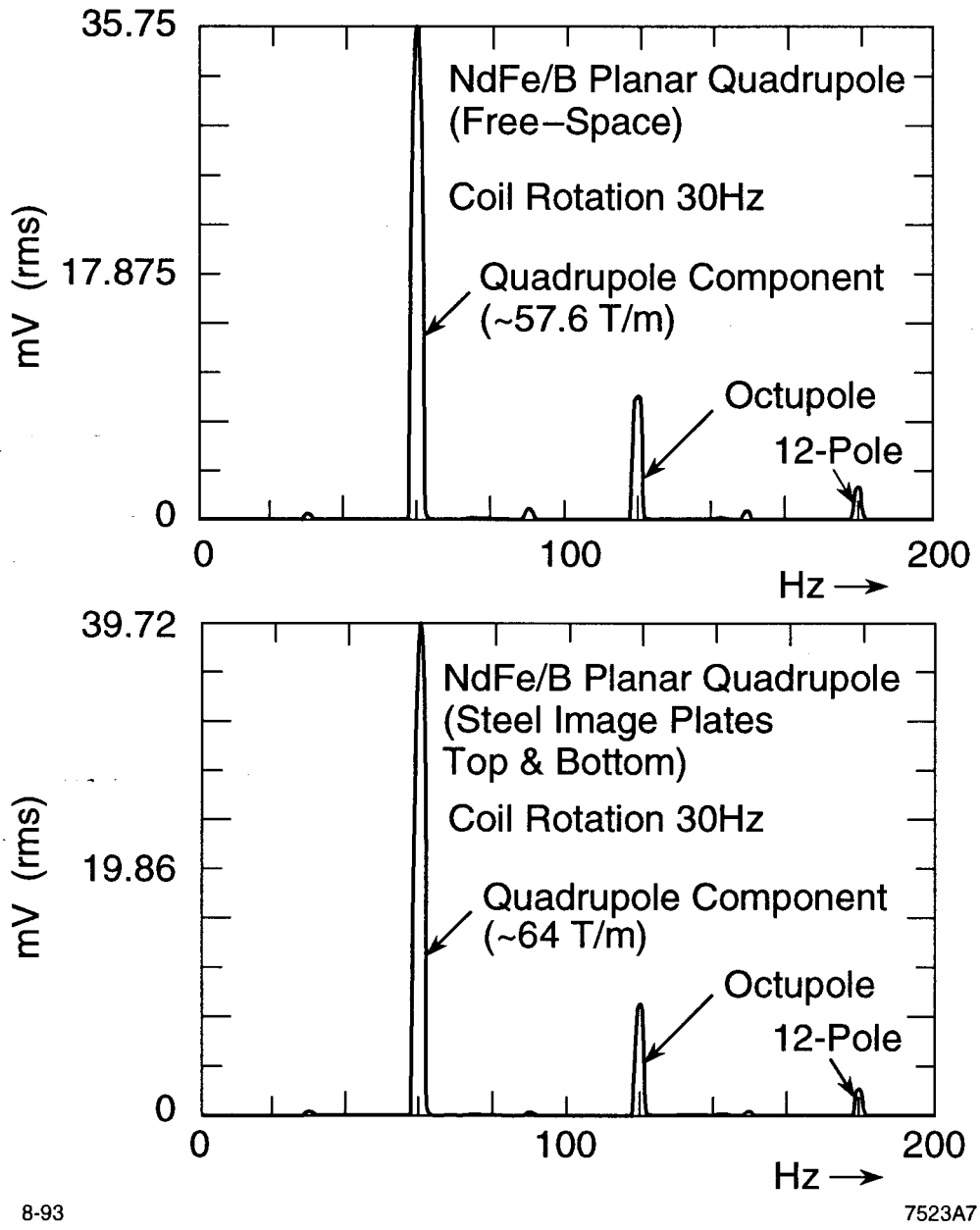
35.75
17.875
0
mV (rms)
NdFe/B Planar Quadrupole
(Free–Space)
Coil Rotation 30Hz
Quadrupole Component
(~57.6 T/m)
Octupole
12-Pole
0
100
200
Hz →
39.72
19.86
0
mV (rms)
NdFe/B Planar Quadrupole
(Steel Image Plates
Top & Bottom)
Coil Rotation 30Hz
Quadrupole Component
(~64 T/m)
Octupole
12-Pole
0
100
200
Hz →
8-93
7523A7

Fig. 4

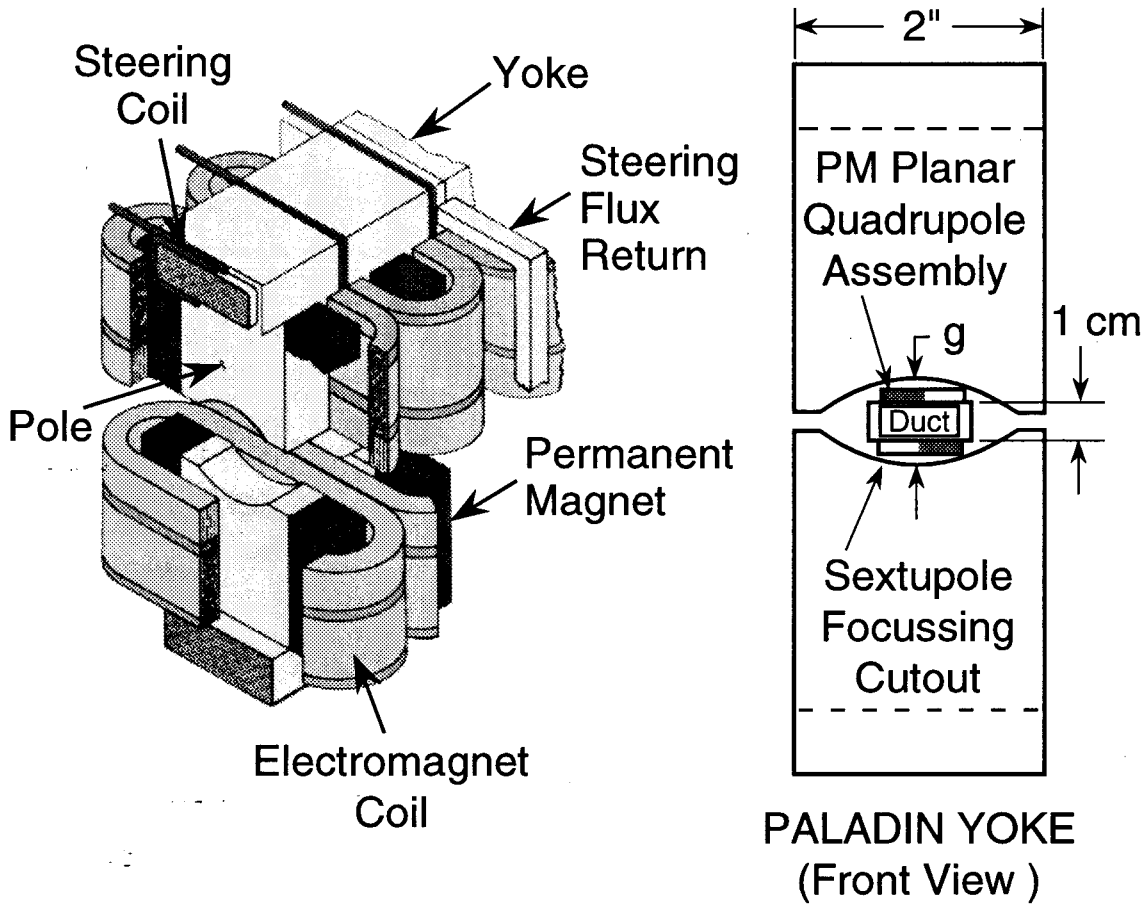
Steering Coil
Yoke
Steering Flux Return
Pole
Permanent Magnet
Electromagnet Coil
2"
PM Planar Quadrupole Assembly
g
1 cm
Duct
Sextupole Focussing Cutout
PALADIN YOKE
(Front View)
8-93
7523A3

Fig. 5

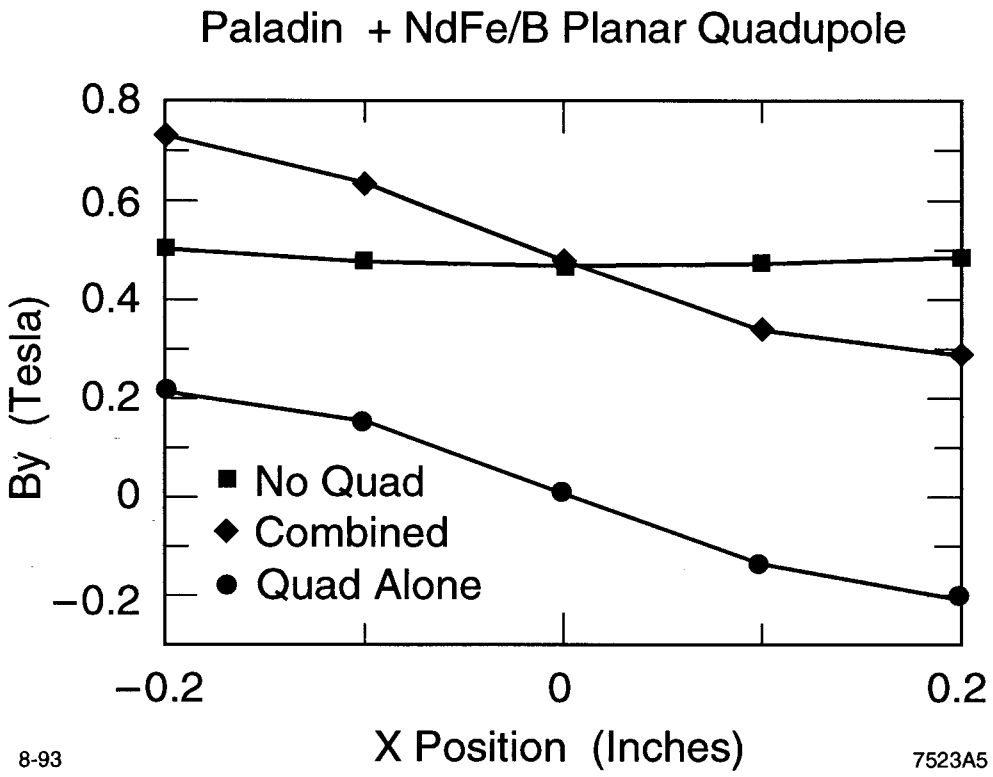
Paladin + NdFe/B Planar Quadupole
0.8
0.6
0.4
0.2
0
−0.2
By (Tesla)
No Quad
Combined
Quad Alone
−0.2
0
0.2
X Position (Inches)
8-93
7523A5

Fig. 6